

11. LATE CENOZOIC ICE-RAFTING RECORDS FROM LEG 145 SITES IN THE NORTH PACIFIC: LATE MIocene ONSET, LATE PLIOCENE INTENSIFICATION, AND PLIOCENE-PLEISTOCENE EVENTS¹

Lawrence A. Krissek²

ABSTRACT

Ice-raftered debris (IRD) in marine sediments provides a valuable direct indicator of the presence of glacial ice at sea level on surrounding continents, and is therefore a useful tool in paleoclimatic studies. The location of sites drilled during Ocean Drilling Program Leg 145, combined with the length, stratigraphic integrity, and good age control of the sediments recovered, provides an opportunity to examine the Late Cenozoic record of North Pacific ice rafting at locations within a few hundred kilometers of potential IRD sources.

Ice-rafting records for Sites 881, 883, and 887 have been determined, with temporal resolution ranging from one sample per 10 k.y. to one sample per 50 k.y. The mass accumulation rate (MAR) of IRD in the coarse sand-sized fraction of each sample has been calculated from the abundance of coarse sand (wt%), the IRD abundance within the coarse sand fraction (vol%), shipboard measurements of sediment dry-bulk density, and average sedimentation rates constrained by shipboard paleomagnetic and biostratigraphic data.

The oldest occurrences of IRD in Leg 145 cores are at least late Miocene in age, and variations in IRD MARs prior to 2.6 Ma are consistent with interpretations of an older episode of tidewater glaciation (~6 to ~4.2 Ma) and a mid-Pliocene warm interval (~4.2 to ~3.0–3.5 Ma) recorded in the Yakataga Formation of coastal Alaska. The age of initial IRD input is younger at Deep Sea Drilling Project (DSDP) sites farther south. IRD MARs at all three sites increase markedly at 2.6 Ma, recording the onset of continental-scale glaciation in the Northern Hemisphere. An accompanying increase in the abundance of volcanic ash may indicate a linkage between volcanism and climate that merits additional study.

Pliocene–Pleistocene IRD MARs decrease from the Gulf of Alaska towards the west and from the northwesternmost Pacific towards the east, which identifies the Alaskan coast and the Kurile/Kamchatka margin as major IRD sources. At least eight episodes of increased IRD MARs can be correlated among Leg 145 sites, and most of these can be correlated to IRD records from DSDP Sites 579 and 580. These increases also correlate to North Pacific-wide episodes described previously, indicating that the Leg 145 IRD MAR records contain the major features of North Pacific paleoclimatic history.

Pliocene–Pleistocene IRD MAR fluctuations at Sites 881 and 887 exhibit quasi-periodic cyclicity with average durations near orbital values. These results suggest that additional high-resolution studies of sediments from Sites 881 and 887 may yield the first North Pacific IRD records comparable in detail to IRD records from the North Atlantic.

INTRODUCTION

In marine sedimentary sequences deposited away from a continental margin and at mid to high latitudes, the presence of anomalously coarse-grained (sand-sized and larger) terrigenous clasts within a finer grained pelagic or hemipelagic matrix provides a valuable direct indicator of the effect of sediment transport by floating ice. As a result, the stratigraphic distribution of such dropstones (i.e., ice-rafted detritus or IRD) can be used to identify times when continental glaciers extended to sea level, whereas the geographic distribution and the composition of the IRD can be used to locate the glaciated source areas. Sediments recovered during Ocean Drilling Program (ODP) Leg 145 from the North Pacific contain IRD, and potentially carry valuable records of the Late Cenozoic glacial history of the Northern Hemisphere; the examination of those records is the objective of this study. The sediments recovered during Leg 145 are particularly suitable for this work because: (1) essentially complete and undisturbed upper Miocene through Pleistocene sections were recovered at each site (Rea, Basov, Janecek, Palmer-Julson, et al., 1993); (2) well-constrained magneto- and biostratigraphies were constructed for each Pliocene–Pleistocene section from shipboard data, and will eventually be supplemented by shore-based paleomagnetic, biostratigraphic, and isotopic studies; and (3) Leg 145 sites are located in a transect across the North Pacific (Fig. 1), ranging from a site near a

potential source of IRD in the Kurile-Kamchatka region (Site 881), through an ice-distal location at Detroit Seamount (Site 883), to a site located near potential IRD sources surrounding the Gulf of Alaska (Site 887).

Previous studies of IRD in the North Pacific have examined materials recovered during Deep Sea Drilling Project (DSDP) Leg 19 (Stewart et al., 1973; Fullam et al., 1973), during Leg 18 (von Heune et al., 1973, 1976), from piston cores (Conolly and Ewing, 1970; Kent et al., 1971), and during DSDP Leg 86 (Krissek et al., 1985). Conolly and Ewing (1970) used coarse-fraction data from 22 *Vema* piston cores to delineate the horizontal and vertical distribution of IRD in the northwest Pacific Ocean. In these samples, the first IRD is younger than approximately 2.2 Ma, IRD becomes common in sediments younger than 1.5 Ma, and IRD is abundant in sediments younger than 1.0 Ma. Limited magneto- and biostratigraphic data prevented the development of a detailed IRD chronology. Geographic distribution and composition of the IRD were interpreted (Connelly and Ewing, 1970) to indicate IRD source areas in the Kurile-Kamchatka-Aleutian arc, with dispersal by a Pleistocene current system similar to the one now in the area. Kent et al. (1971) used coarse-fraction data and detailed paleomagnetic, biostratigraphic, and tephrochronologic age control from nine piston cores to construct a generalized chronology of relative ice-rafting importance in the North Pacific. This chronology includes four periods of increased ice-rafting between 1.2 and 2.5 Ma, and at least 11 such intervals from 1.2 Ma to the present.

IRD studies of sediments recovered during DSDP Legs 19 (Stewart et al., 1973; Fullam et al., 1973) and 18 (von Heune et al., 1973, 1976) were hampered by the discontinuous and limited recovery of the cored sections. As demonstrated by von Heune et al. (1973): (1) the abun-

¹ Rea, D.K., Basov, I.A., Scholl, D.W., and Allan, J.F. (Eds.), 1995. *Proc. ODP, Sci. Results*, 145: College Station, TX (Ocean Drilling Program).

² Department of Geological Sciences, The Ohio State University, 130 Orton Hall, So. Oval, Columbus, OH 43210, U.S.A.

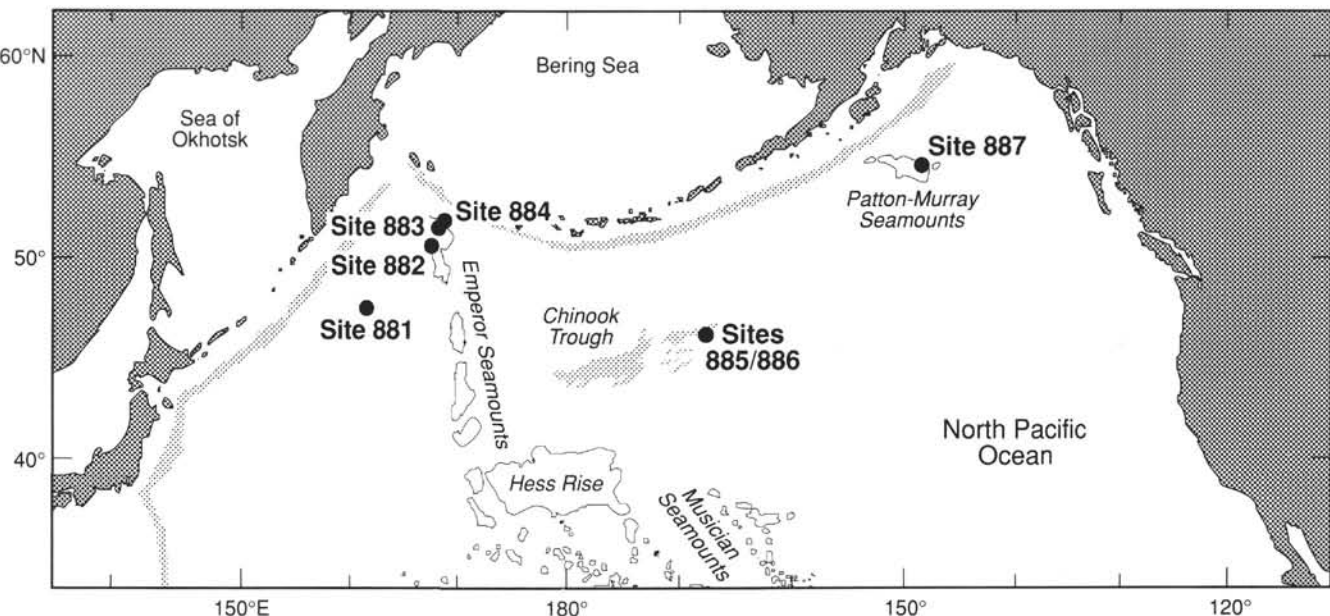


Figure 1. Location map of ODP Leg 145 sites in the North Pacific Ocean. From Rea, Basov, Janecek, Palmer-Julson, et al. (1993).

dance of the coarse sand fraction ($250 \mu\text{m}$ – 2 mm) in the Gulf of Alaska is an accurate indicator of IRD abundance, and (2) periods of IRD influx lasted approximately 10,000 to 20,000 years. In subsequent work, von Heune et al. (1976) used data from Site 178 and a piston core to construct an IRD chronology for the past 300 k.y. in the Gulf of Alaska; this chronology correlates positively with variations in other Northern Hemisphere climatic indicators during the same period.

At DSDP Sites 579 and 580, located in the northwest Pacific, IRD abundances are generally lower than in the study areas located farther north and east (Krissek et al., 1985). Despite this limitation, IRD first appears at Sites 579 and 580 at approximately 2.6 Ma, the importance of IRD increases in sediments deposited since approximately 1.0 Ma, and peaks in IRD importance since 1.0 Ma are generally synchronous with periods of major ice rafting throughout the North Pacific (as defined by Kent et al., 1971). In contrast to the findings of von Heune et al. (1973), the coarse-sand fraction at Sites 579 and 580 contains a significant non-IRD component, so that the abundance of the coarse-sand fraction is not an accurate indicator of IRD abundance. Instead, both the abundance and the composition of the coarse sand fraction must be known to accurately define the spatial and temporal distribution of IRD.

Although the details of these previous studies differ (e.g., continuity of core recovery, temporal resolution of sampling, grain size of sediment designated as IRD), the general conclusions of these studies are consistent and can be summarized as follows:

1. The abundance of terrigenous coarse-grained material does indicate the relative importance of ice rafting at the time of deposition.
2. The IRD has been transported predominantly from major source areas on the perimeter of the Gulf of Alaska and along the Kurile-Kamchatka margin, so that IRD is most common at locations in the Gulf of Alaska and the northwestern Pacific. IRD occurrences/abundances decrease from these locations toward the central part of the northernmost Pacific, and also decrease to the south at approximately all longitudes.
3. The temporal record of ice rafting includes limited dropstone occurrences prior to approximately 2.6 Ma, and significant increases in IRD abundance at approximately 2.6 Ma (Rea and Schrader, 1985) and 1.0 Ma. This record is interpreted to record the relatively limited extent of Northern Hemisphere glaciation prior to approximately 2.6 Ma, the onset of significant continent-scale Northern Hemisphere gla-

ciation at approximately 2.6 Ma, and the apparent intensification of Northern Hemisphere climatic fluctuations since approximately 1.0 Ma.

Recent studies of Miocene and younger strata from the perimeter of the northernmost Pacific have provided additional insight into the late Miocene and Pliocene climatic history of the region; this record is consistent with the pre-Pleistocene paleoclimatic history constructed previously from marine cores. The oldest IRD found in the Yakataga Formation, which is exposed around the Gulf of Alaska, is dated at approximately 6 Ma, and sedimentologic and paleontologic data indicate significant tidewater glacial effects from approximately 6 Ma to approximately 4.2 Ma (termed "Glacial A"; Lagoe et al., 1993). Microfossil assemblages and reduced IRD abundances in the Yakataga Formation indicate a relatively warm mid-Pliocene interval from approximately 4.2 Ma to sometime between 3.5 and 3.0 Ma (Lagoe et al., 1993); the effects of this mid-Pliocene warm interval have also been recognized by Gladenkov et al. (1991) from mollusc, ostracode, and benthic foraminiferal assemblages at Karaginsky Island in eastern Kamchatka. A younger cooling episode ("Glacial B" in the Yakataga Formation; Lagoe et al., 1993) begins between 3.0 and 3.5 Ma in both records, with substantial cooling evident at approximately 2.5 to 2.6 Ma.

Sediments recovered during Leg 145 provide a unique opportunity to test the proposed Late Cenozoic glacial history of the circum-North Pacific by using IRD records from continuous, undisturbed, and well-dated marine sections. As a result, this study will examine evidence for the onset of ice-rafting in the late Miocene and for paleoclimatic fluctuations within the Pliocene–Pleistocene. Because of shipboard sampling and time constraints, this study is a reconnaissance examination of the IRD records from three of the Leg 145 sites. Future high-resolution studies, combined with the potential for oxygen isotope stratigraphies from Detroit Seamount (Site 883) and Patton-Murray Seamount (Site 887), may provide the first opportunity to correlate the North Pacific IRD record directly to isotopically calibrated paleoclimatic records from other parts of the world.

MATERIALS AND METHODS

Samples for IRD analysis were taken at regularly spaced intervals from the continuously cored upper Miocene, Pliocene, and Pleistocene sections of Sites 881, 883, and 887. The depth ranges sampled, spacing between samples, average sedimentation rates, and resulting

temporal resolution of sampling are summarized in Table 1. The sedimentation rates used to calculate sample ages are average interval sedimentation rates defined by shipboard paleomagnetic and biostratigraphic datums, and have previously been used to estimate mass accumulation rates (MARs) of individual sediment components (Rea, Basov, Janecek, Palmer-Julson, et al., 1993). Shore-based biostratigraphic and isotopic data may result in significant revisions of these age-depth models. As indicated in Table 1, the temporal resolution of these samples is appropriate for identifying relatively long-term climatic trends, but is not appropriate for identifying short-term fluctuations (e.g., short orbital periodicities or Atlantic-type "Heinrich" events). Additional high-resolution sampling and improved age control will be required to identify such short-term fluctuations.

Complete descriptions of the lithologic units sampled at each site are given in Rea, Basov, Janecek, Palmer-Julson, et al. (1993), but the major characteristics of those units are summarized briefly here. At Site 881 (Fig. 1), samples were taken from the youngest lithologic unit, Unit I, which consists of 364 m of diatom ooze and clayey diatom ooze. Lithologic Unit I at Site 881 is subdivided into two subunits, based on a downcore decrease in terrigenous content and the absence of volcanic ash in the lower subunit. The boundary between the two subunits at Site 881 (163 m below seafloor [mbsf]) coincides with the Matuyama/Gauss paleomagnetic boundary (dated at 2.6 Ma). The oldest sediments from Site 881 sampled for this study are dated as late Miocene (approximately 7 Ma).

At Site 883 (Fig. 1), samples were taken from lithologic Unit I and the underlying lithologic Unit II. Lithologic Unit I is composed of 87 m of clay with diatoms, diatom ooze, and diatom clay, with abundant volcanic ash. Lithologic Unit II is composed of 371 m of diatom ooze, with very little volcanic ash. The boundary between Unit I and Unit II lies just below the Matuyama/Gauss paleomagnetic boundary. The oldest sediments from Site 883 sampled for this study are dated as late Miocene (approximately 5 Ma).

At Site 887 (Fig. 1), samples were taken from lithologic Unit I and the underlying lithologic Unit II. Lithologic Unit I is composed of 90 m of siliceous silty clay mixed sediments, diatom ooze, and clay, with abundant volcanic ash. Lithologic Unit II is composed of 180 m of diatom ooze and a variety of minor lithologies, with less volcanic ash than is present in Unit I. The boundary between lithologic Units I and II lies just below the Matuyama/Gauss paleomagnetic boundary. The oldest sediments from Site 887 sampled for this study are dated as late Miocene (approximately 5.5 Ma).

On the basis of previous studies in the North Pacific (von Heune et al., 1973, 1976; Krissek et al., 1985), the 250 μm -2 mm grain-size interval was chosen as the indicator of IRD abundance. Samples were dried at 60°C, weighed, disaggregated ultrasonically, and wet-sieved at 2 mm and 250 μm . The 250 μm -2 mm size fraction was then dried and weighed, and the abundance of the coarse-sand fraction (weight %) was calculated. The coarse-sand fraction of each sample was examined under a binocular microscope, and the abundance of terrigenous, nonvolcanic clasts (volume %) was estimated. The MAR of coarse sand-sized IRD was then estimated as

$$\text{IRD MAR} = \text{CS}\% \times \text{IRD}\% \times \text{DBD} \times \text{LSR},$$

where IRD MAR is the mass accumulation rate ($\text{g}/\text{cm}^2/\text{k.y.}$), CS% is the coarse-sand abundance (weight %), IRD% is the IRD abundance in the coarse-sand fraction (volume %), DBD is the dry-bulk density of the sediment (g/cm^3), and LSR is the interval average linear sedimentation rate ($\text{cm}/\text{k.y.}$).

All values used in these calculations are given in the Appendix (this chapter). Dry-bulk densities were obtained from the tables of discrete physical properties measurements in the appropriate chapters of Rea, Basov, Janecek, Palmer-Julson, et al. (1993). The dry-bulk density value chosen for each sample is the value of the closest (either overlying or underlying) discrete measurement. Linear sedimentation rates are the average interval values used to calculate component

Table 1. Summary of depth ranges sampled, sample spacing, linear sedimentation rates,* and resultant temporal sampling interval at Sites 881, 883, and 887.

Site	Depth (mbsf)	Sample spacing (cm)	Sedimentation rate (cm/k.y.)	Temporal sample spacing (k.y.)
881	0–108	150	5.4	28
	108–163	150	9.3	16
	163–220	150	3.4	44
	220–286	75–150	5.4	14–28
883	286–334	75–150	3.0	25–50
	0–86	150	3.3	45
	86–168	150	9.1	16
887	168–300	450	9.1	49
	0–56	50	5.4	10
	57–87	50	2.0	25
	87–163	50	2.6	19

Note: *Rea, Basov, Janecek, Palmer-Julson, et al. (1993).

fluxes in the appropriate chapters of Rea, Basov, Janecek, Palmer-Julson, et al. (1993).

In this study, the IRD MAR, rather than the IRD abundance (wt%), is used as an indicator of IRD supply through time. IRD MAR is the preferred indicator because the MAR of an individual component, such as IRD, is independent of the supply rates of other components, such as volcanic ash or biogenic material. It should be noted, however, that the IRD MAR calculated in this study may underestimate the actual IRD MAR, because the density of IRD is higher than the densities of biogenic material (diatoms, radiolarians, foraminifera) and volcanic ash. The IRD MAR calculated for a sample composed only of IRD will be the actual IRD MAR, but the IRD MAR calculated for a sample containing a mixture of IRD and biogenic components will underestimate the mass contribution from IRD if the volume abundance is not corrected for differences in the densities of the components. In this data set, such underestimates are more important in the deeper (older) parts of the records, where IRD is a minor volumetric constituent (but the major contributor of mass) in biogenically dominated samples. Coarse-sand abundances are generally very low in the older samples, however, so that increasing the IRD contribution to the coarse-sand abundance still would not significantly change the overall pattern of IRD MAR fluctuations observed at these sites.

DATA

IRD abundances and MARs are tabulated in the Appendix. The abundance of IRD (weight %) at Sites 881, 883, and 887 is plotted as a function of depth downcore in Figure 2, and IRD MAR profiles for each site are shown in Figures 3 and 4. IRD abundances at Site 881 (Fig. 2A) range between 0 and 6 wt%, with a distinct shift in the record at 163 mbsf. Above that level, IRD abundances generally fall between 0.5 and 3.0 wt%, whereas most abundances below 163 mbsf are very close to zero. The corresponding change on the MAR profiles (Figs. 3A and 4A) occurs at 2.6 Ma, from approximately $0 \text{ g}/\text{cm}^2/\text{k.y.}$ to values generally between 0.03 and $0.09 \text{ g}/\text{cm}^2/\text{k.y.}$ Maximum IRD MAR values are approximately $0.21 \text{ g}/\text{cm}^2/\text{k.y.}$ at Site 881. Most of the fluctuations in the IRD MAR record younger than 2.6 Ma include at least one data point intermediate between the maximum and minimum values, suggesting that these fluctuations are not simply an artifact of the sampling interval. As a result, these fluctuations may provide a hint of underlying cyclicity within this record.

IRD abundances at Site 883 (Fig. 2B) range between 0 and 0.7 wt%, with a distinct shift in the record at 82 mbsf. Above that level, IRD abundances are generally between 0.1 and 0.6 wt%, whereas most abundances below 82 mbsf are very close to zero. The corresponding change on the MAR profiles (Figs. 3B and 4B) occurs at approximately 2.5 Ma, from approximately $0 \text{ g}/\text{cm}^2/\text{k.y.}$ to values generally between 0.001 and $0.008 \text{ g}/\text{cm}^2/\text{k.y.}$ The magnitude of IRD MAR maxima

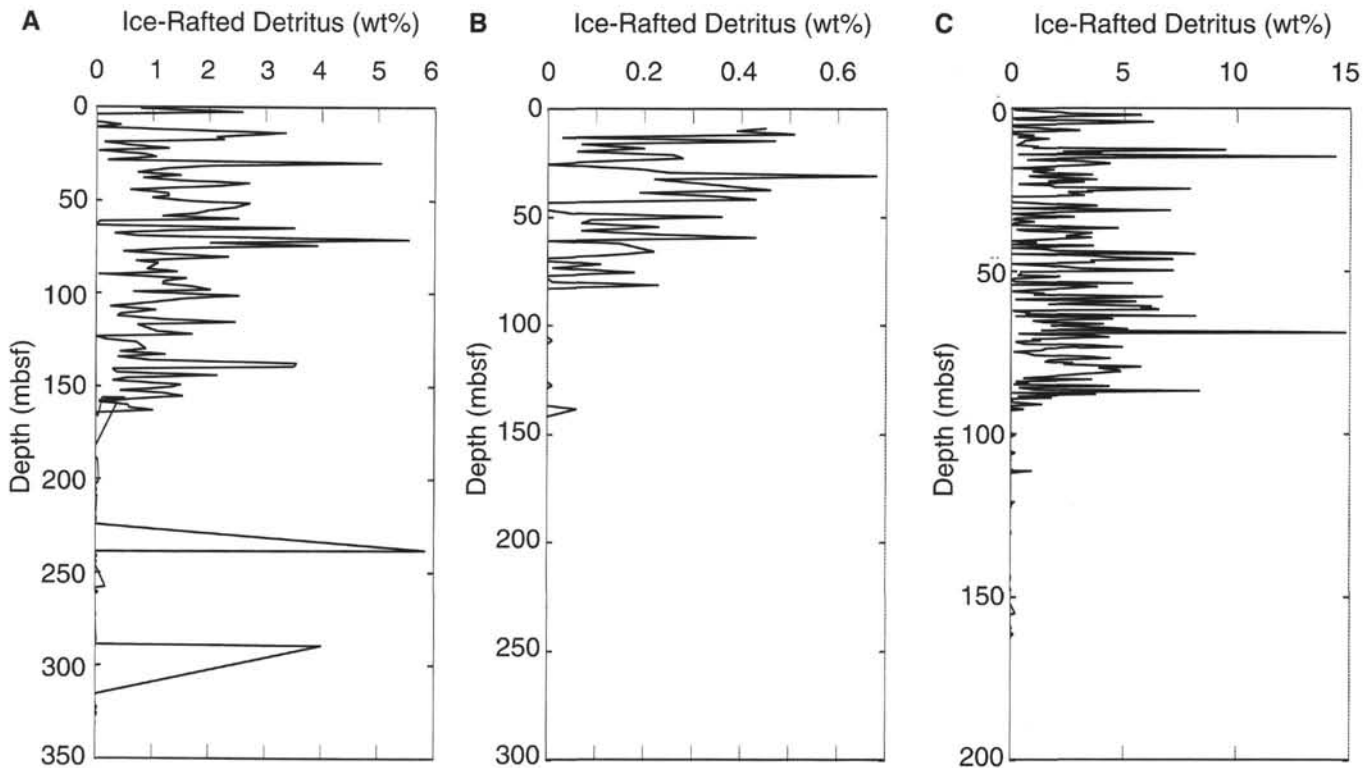


Figure 2. Abundance of coarse sand-sized ($250 \mu\text{m}$ – 2 mm) IRD as a function of depth (mbsf). Note change in abundance scales between plots. A. Data for Site 881. B. Data for Site 883. C. Data for Site 887.

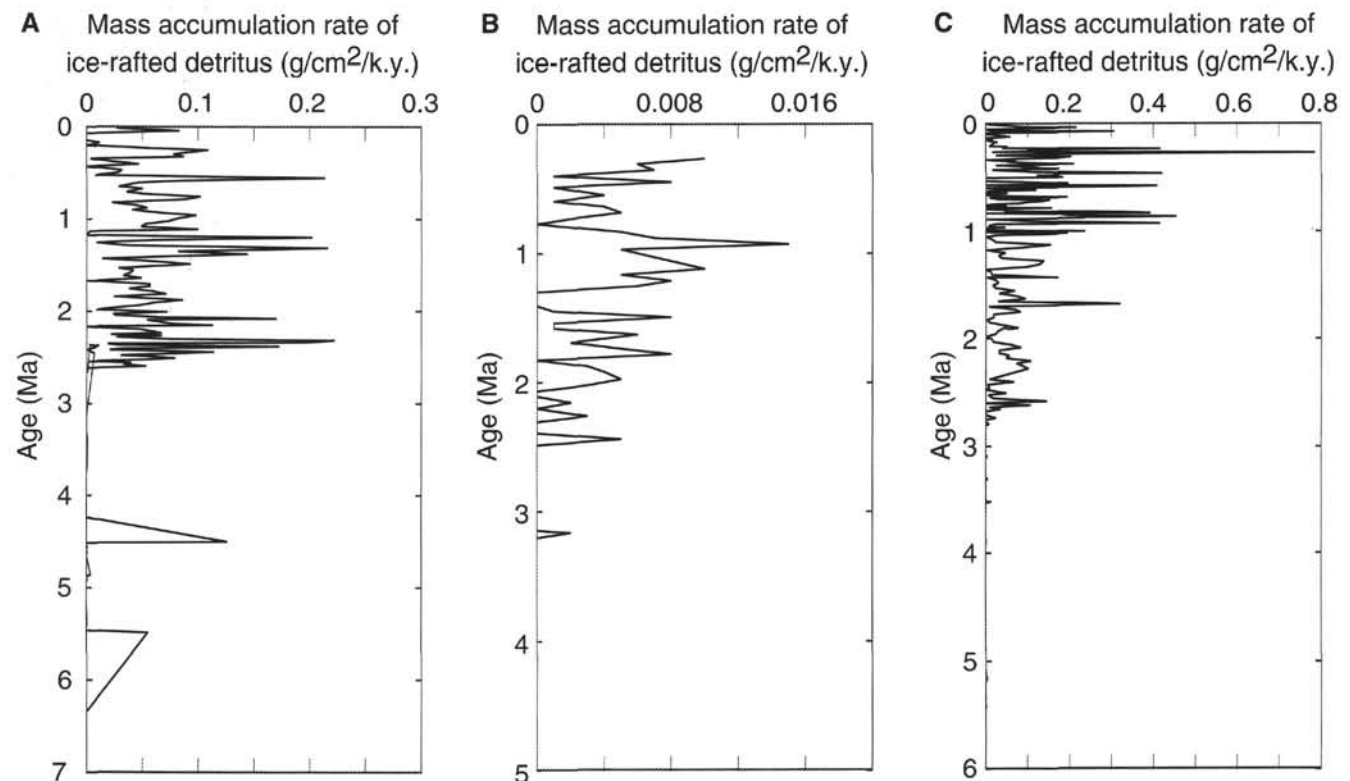


Figure 3. Mass accumulation rate of coarse sand-sized IRD as a function of sediment age for entire record analyzed at each site. Note change in abundance scales between plots. MARs increase at each site at approximately 2.6 Ma. A. Data for Site 881. B. Data for Site 883. C. Data for Site 887.

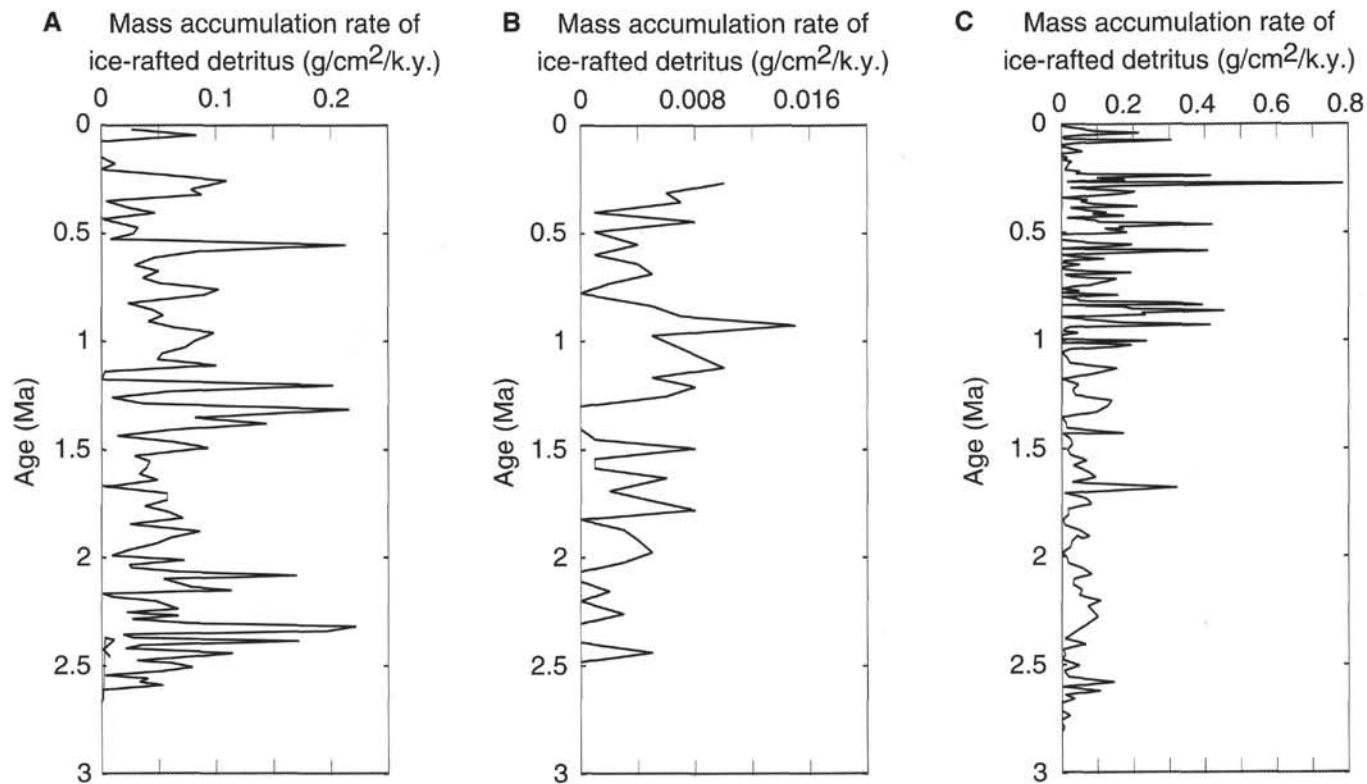


Figure 4. Mass accumulation rate of coarse sand-sized IRD as a function of sediment age for the interval 0–3 Ma. Note change in abundance scales between plots. Note the quasi-periodic fluctuations between 0 and 2.0 Ma at Site 881, and between 0 and 1.0 Ma at Site 887. **A.** Data for Site 881. **B.** Data for Site 883. **C.** Data for Site 887.

generally increases from 2.5 to 1.0 Ma, decreases sharply from 1.0 to approximately 0.7 Ma, and then increases in sediments younger than 0.7 Ma. Most peaks in the Site 883 IRD MAR record are defined by single points at the corresponding maximum and minima, probably because of the relatively long sample spacing in this data set. As a result, the details of this record (as presently shown in Figs. 3B and 4B) are probably more an artifact of the sample spacing than an indicator of actual short-term variations in the IRD MAR.

IRD abundances at Site 887 (Fig. 2C) range between 0 and 15 wt%, with a distinct shift in the record at approximately 88 mbsf. Above that level, IRD abundances range between 0 and 15 wt%, whereas most abundances below 88 mbsf are very close to zero. The corresponding change on the MAR profiles (Figs. 3C and 4C) occurs at 2.6 Ma, from approximately 0 $\text{g}/\text{cm}^2/\text{k.y.}$ to values generally between 0.0 and 0.20 $\text{g}/\text{cm}^2/\text{k.y.}$ Maximum IRD MAR values at Site 887 are approximately 0.40 $\text{g}/\text{cm}^2/\text{k.y.}$ Many of the MAR peaks younger than 2.6 Ma, and especially those younger than 1.0 Ma, are defined by the two minima, the maximum, and several intermediate values, suggesting that these fluctuations are not an artifact of the sampling interval. Instead, these fluctuations suggest that short-term cyclicity is a real attribute of the IRD MAR record at Site 887, making this site an obvious candidate for future high-resolution studies.

DISCUSSION

The data presented in Figures 2, 3, and 4, as well as observations of pebble- to cobble-sized dropstones in the shipboard core descriptions (Rea, Basov, Janecek, Palmer-Julson, et al., 1993), indicate that IRD ranges from present to abundant in the upper Miocene through Pleistocene sections cored during Leg 145. The records of ice-rafting investigated here provide strong evidence of a major increase in the effects of glaciation at 2.6 Ma, consistent with the results of previous IRD studies in the North Pacific and with a variety of paleoclimatic signals

from elsewhere in the Northern Hemisphere. These relatively long and continuous records also provide valuable information about both the early history of late Cenozoic glaciation in the circum-North Pacific and the general patterns of glaciation since approximately 2.6 Ma. In addition, these records provide preliminary suggestions of short-term glacial fluctuations since 2.6 Ma; this aspect of the IRD MAR record should be examined by high-resolution studies in the future.

Ice-rafting and Glaciation prior to 2.6 Ma

Intervals of ice-rafting prior to 2.6 Ma can be identified by the presence of peaks in the MAR of coarse sand-sized IRD, as well as by the occurrences of macroscopic IRD recorded in the shipboard descriptions of the cores. At Site 881, this “older” coarse sand-sized IRD was deposited at 6.6, 5.5, 4.8–4.9, 4.5–4.6, 4.2, 3.9, 3.8, and 3.4–3.7 Ma, and macroscopic IRD was observed in sediments deposited at approximately 4.6 and 4.2 Ma. The occurrences younger than 4.2 Ma are relatively minor, however, with each based on the presence of a single terrigenous grain in a single sample. As a result, the record from Site 881 is consistent with previous observations of early glacial effects from 6 Ma to approximately 4.2 Ma, followed by a mid-Pliocene warm interval with reduced glacial effects from approximately 4.2 Ma to approximately 3.0–3.5 Ma (Gladenkova et al., 1991; Lagoe et al., 1993).

At Site 883, the only occurrence of “older” coarse sand-sized IRD was deposited at approximately 3.17 Ma, and the only potential macroscopic dropstones occur in sediments deposited at approximately 3.0 Ma. In Hole 883B, a limestone of this age is described as “pumice” (Rea, Basov, Janecek, Palmer-Julson, et al., 1993), whereas the lithology of a limestone of the same age in Hole 883C is not described. As a result, it is unclear whether these macroscopic clasts are ice rafted or not. Despite this uncertainty, however, it is clear that Site 883 received little IRD at any time prior to 2.6 Ma.

At Site 887, "older" coarse sand-sized IRD was deposited at 5.3–5.4, 5.2, 4.9, 4.3–4.4, 3.7–3.9, 3.5–3.6, 3.3–3.4, and 3.1 Ma, and macroscopic IRD was observed in sediments deposited at approximately 4.5 and 3.9 Ma. This distribution of IRD spans both the older glacial episode and the mid-Pliocene warm interval identified in the Yakataga Formation by Lagoe et al. (1993). The IRD distribution at Site 887 may extend into the younger glacial episode of the Yakataga Formation, depending on the actual time of transition from the mid-Pliocene warm interval to the younger glacial (estimated at 3.0–3.5 Ma by Lagoe et al., 1993). The presence of IRD in sediments older than approximately 4.2 Ma is consistent with the presence of tide-water glaciers that deposited the older glacial interval in the Yakataga Formation. The presence of IRD in sediments deposited at Site 887 during the mid-Pliocene warm interval is not inconsistent with observations from the Yakataga Formation, because IRD is observed in the mid-Pliocene warm interval of that unit, although in lower abundances than in the glacial intervals (Lagoe et al., 1993).

The IRD MAR data presented here, together with the observations of macroscopic IRD, indicate that ice-rafting began by 5.5–6.0 Ma in both the Alaskan and Kurile/Kamchatka IRD sources. The first appearance of IRD at a particular site in the North Pacific also depends on the geographic location of that site, however, because the age of first IRD appearance generally decreases toward the south. In particular, Krissek et al. (1985) identified the oldest IRD at DSDP Sites 579 and 580 (approximately 500 km south of Site 881) as late Pliocene in age, and a single pebble of quartz schist, possibly ice rafted, is recorded in upper Pliocene sediments at DSDP Site 177 (approximately 400 km south of Site 887; Kulm, von Heune, et al., 1973).

Onset of Significant Glaciation and Ice-rafting

In each of the three IRD MAR records analyzed here, as well as in the general distribution of macroscopic IRD in Leg 145 cores, the importance of ice-rafter material increases dramatically at, or very close to, the Matuyama/Gauss paleomagnetic boundary (2.6 Ma on the time scale of Cande and Kent, 1992). A similar age for the first appearance of significant IRD was previously reported for the North Pacific (Kent et al., 1971; Krissek, et al., 1985; Rea and Schrader, 1985), the North Atlantic (Shackleton et al., 1984; Ruddiman, McIntyre, and Raymo, 1987; Raymo et al., 1987), and the Norwegian Sea (Krissek, 1989; Jansen et al., 1990; Jansen and Sjøholm, 1991). This increase has generally been interpreted as recording the onset of continental-scale glaciation in the Northern Hemisphere. Limited amounts of IRD found in sediments older than 2.6 Ma around the perimeter of the North Pacific (this study and Lagoe et al., 1993), in the Irminger Basin off southeastern Greenland (Larsen et al., 1994), and in the Norwegian Sea (Krissek, 1989; Jansen et al., 1990; Jansen and Sjøholm, 1991) indicate initial glaciation prior to 2.6 Ma, but a variety of data types from throughout the Northern Hemisphere indicate a major change in Northern Hemisphere paleoclimates at approximately 2.6 Ma (e.g., Raymo et al., 1989).

Although this glacial intensification at approximately 2.6 Ma in the Northern Hemisphere is widely recognized, causes for this change remain speculative. One set of explanations has focused on the possible modification of Northern Hemisphere atmospheric circulation by late Neogene uplift in southeastern Asia and southwestern North America (Ruddiman, Raymo, and McIntyre, 1986; Ruddiman and Raymo, 1988). Another set of explanations has proposed linkages between increased rates of uplift in the late Neogene, increased rates of chemical weathering, and decreased levels of atmospheric and oceanic CO₂ (Raymo et al., 1988; Hodell et al., 1989; Raymo and Ruddiman, 1992). An older proposal (Kennett and Thunell, 1975) suggested a relationship between increased volcanic activity (as recorded by increased amounts of volcanic ash in marine cores) at this time and climatic deterioration, although the details of this relationship were not discussed. Although data from Leg 145 can add only a small piece to this puzzle, these cores do show essentially synchro-

nous increases in the abundance of volcanic ash (used to define the youngest lithologic units at Sites 881, 883, and 887) and in IRD MAR at approximately 2.6 Ma. This association suggests that linkages between volcanism and the glacial record should be reconsidered, especially since both records may be related to tectonic activity in the area. High-resolution studies of Sites 881 and/or 887 are planned to further examine these potential linkages.

Spatial Patterns of Pliocene–Pleistocene Ice-rafting

In sediments younger than 2.6 Ma, the IRD MAR maxima are largest at Site 887 (averaging approximately 0.20 g/cm²/k.y.), intermediate at Site 881 (averaging approximately 0.07 g/cm²/k.y.), and smallest at Site 883 (averaging approximately 0.006 g/cm²/k.y.). This spatial pattern indicates that major ice sources were located on the perimeter of the Gulf of Alaska and along the Kurile/Kamchatka margin, as interpreted previously by Conolly and Ewing (1970). Provenance studies of the Leg 145 IRD are discussed elsewhere (McKelvey, this volume), but the low IRD MARs at Site 883 indicate either that few icebergs were transported from these sources to the vicinity of Site 883 (Detroit Seamount), or that icebergs passing through the area experienced little melting because of cool surface waters within an expanded Subarctic Gyre. Direct evidence to distinguish between these two possibilities will require microfossil-based reconstructions of sea-surface temperatures at these sites.

Temporal Patterns of Pliocene–Pleistocene Ice-rafting

At least eight episodes of increased IRD MARs can be correlated among two or more Leg 145 sites (Fig. 5); this degree of agreement is surprisingly good, considering both the differences in the sampling intervals at Sites 881, 883, and 887, and the uncertainties introduced by using average interval sedimentation rates to calculate sample ages. Most of these eight episodes can be correlated farther south and west to peaks in the IRD abundance records from DSDP Sites 579 and/or 580 (Krissek et al., 1985). The times of increased ice rafting at approximately 1.09–1.13, 0.92–0.93, 0.76–0.79, 0.68–0.69, 0.55–0.56, 0.31–0.32, 0.27–0.29, and 0.02–0.05 Ma correlate well with North Pacific-wide periods of increased ice rafting previously identified by Kent et al. (1971) and by von Heune et al. (1976). Two periods of a relatively lower amplitude increase, which were identified by Kent et al. (1971), are not seen in the Leg 145 data. Despite the absence of these two smaller IRD peaks, the strong general correlation between the Leg 145 data sets and the detailed data of Kent et al. (1971) indicates that the major features of North Pacific paleoclimatic history are represented in the Leg 145 records.

The relatively low temporal resolution of the Leg 145 IRD MAR records and the uncertainties in the present age-depth models for these sites preclude a detailed analysis of short-term (e.g., orbital-scale) cyclicity at this time. The Pliocene–Pleistocene IRD MAR records from Sites 881 and 887, however, do exhibit quasi-periodic fluctuations with average durations near orbital values (i.e., the 19 k.y. and 23 k.y. precessional cycles, the 41 k.y. obliquity cycle, and the 100 k.y. eccentricity cycle). For example, between nine and 11 maxima are present in the Site 881 record between 0.0 and 1.0 Ma, and 11 maxima are present between 1.0 and 2.0 Ma; as a result, the average time between maxima is approximately 100 k.y. As another example, between 10 and 12 maxima are present in the Site 887 record between 0.0 and 0.5 Ma, and 10 or 11 maxima are present between 0.5 and 1.0 Ma; as a result, the average time between maxima is approximately 40 to 50 k.y. The presence of such quasi-cyclic fluctuations in these relatively low-resolution records suggests that valuable high-resolution paleoclimatic records, perhaps containing evidence of orbital-scale cyclicity, can be developed by future detailed studies of IRD MARs at Sites 881 and 887. Such high-resolution IRD records would be the first from the North Pacific comparable in detail to those available from the North Atlantic (Shackleton et al., 1984), and would contribute

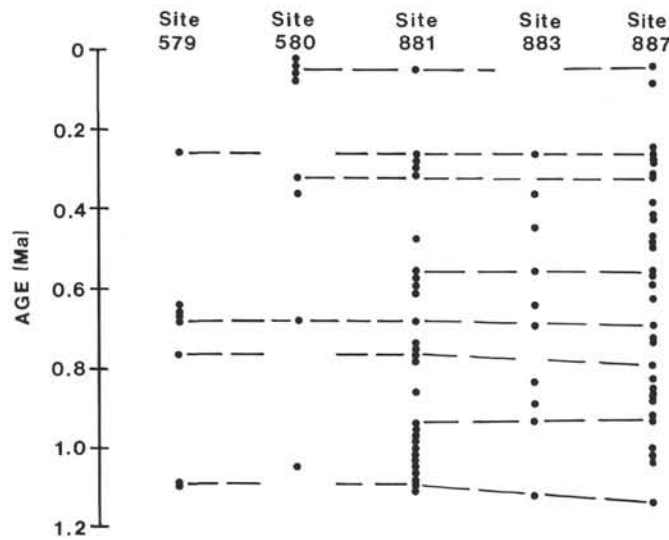


Figure 5. Correlation diagram of times of increased IRD MARs at ODP Sites 881, 883, and 887, and of increased IRD abundance at DSDP Sites 579 and 580 (Krissek et al., 1985). Horizontal dashed lines correlate IRD increases among sites, and correlate with North Pacific-wide episodes of increased ice rafting identified previously by Kent et al. (1971).

significantly to inter-ocean comparisons of behavior during glacial/interglacial fluctuations.

CONCLUSIONS

1. The oldest occurrences of macroscopic IRD and coarse sand-sized IRD in the Leg 145 cores are at least late Miocene in age. IRD occurrences dated between 6.6 and 4.2 Ma in both the northwest Pacific (Site 881) and the Gulf of Alaska (Site 887) correlate with evidence of early tidewater glaciation in the Yakataga Formation of coastal Alaska (Lagoe et al., 1993). IRD supply was reduced during a mid-Pliocene warm interval, which was identified previously from the Yakataga Formation (Lagoe et al., 1993) and outcrops in Kamchatka (Gladenkov et al., 1991). The oldest IRD is younger at locations farther south, with the oldest IRD at DSDP Sites 177, 579, and 580 dated as late Pliocene.

2. The MAR of coarse sand-sized IRD increases markedly at, or close to, the Matuyama/Gauss magnetic boundary (2.6 Ma) at Sites 881, 883, and 887, and records the onset of continental-scale glaciation in the Northern Hemisphere. The abundance of volcanic ash in these cores increases synchronously with the IRD MAR change, suggesting that linkages between volcanism and climate proposed by Kennett and Thunell (1975) should be reconsidered by future high-resolution studies.

3. During the Pliocene–Pleistocene, the major sources of IRD were located around the perimeter of the Gulf of Alaska and along the Kurile/Kamchatka margin; these results agree with the findings of Conolly and Ewing (1970). Because of the location of these sources, IRD MARs are high in the Gulf of Alaska (Site 887) and the northwest Pacific (Site 881), and decrease both toward the center of the northernmost Pacific (Site 883) and toward the south. Microfossil-based reconstructions of sea-surface temperatures will be required to evaluate the roles of iceberg trajectories and preferential melting on the distribution of IRD away from these sources.

4. Within the Pliocene–Pleistocene section, at least eight episodes of increased IRD MARs can be correlated among Leg 145 sites. Most of these episodes also can be recognized at DSDP Sites 579 and 580, and correlate to basin-wide increases described previously by Kent et al. (1971). As a result, the Leg 145 IRD MAR records appear to record the major features of North Pacific paleoclimatic history.

5. At Sites 881 and 887, Pliocene–Pleistocene fluctuations in IRD MARs exhibit quasi-periodic cyclicity with average durations near orbital values (~100 k.y. and ~40 k.y., respectively). These preliminary results suggest that high-resolution studies at these sites may yield the first North Pacific IRD records comparable in detail to IRD records from the North Atlantic.

ACKNOWLEDGMENTS

This work was supported by a post-cruise JOI-USSSP grant. Thanks to Captain Ed Oonk, the SEDCO drilling crew, Ron Grout, and the ODP technical staff for their assistance during Leg 145. T. Gray and K. Kudless provided able assistance in laboratory analysis of these samples. M. Lagoe and C. Eyles provided helpful reviews of this manuscript.

REFERENCES*

- Cande, S.C., and Kent, D.V., 1992. A new geomagnetic polarity time scale for the Late Cretaceous and Cenozoic. *J. Geophys. Res.*, 97:13917–13951.
- Connelly, J.R., and Ewing, M., 1970. Ice-raftered detritus in Northwest Pacific deep-sea sediments. In Hays, J.D. (Ed.), *Geological Investigations of the North Pacific*. Mem.—Geol. Soc. Am., 126:219–231.
- Fullam, T.J., Supko, P.R., Boyce, R.E., and Stewart, R.W., 1973. Some aspects of Late Cenozoic sedimentation in the Bering Sea and North Pacific Ocean. In Creager, J.S., Scholl, D.W., et al., *Init. Repts. DSDP*, 19: Washington (U.S. Govt. Printing Office), 887–896.
- Gladenkov, Y.B., Barinov, K.B., Basilian, A.E., and Cronin, T.M., 1991. Stratigraphy and paleoceanography of Pliocene deposits of Karaginsky Island, eastern Kamchatka, USSR. *Quat. Sci. Rev.*, 10:239–246.
- Hodell, D.A., Mueller, P.A., McKenzie, J.A., and Mead, G.A., 1989. Strontium isotope stratigraphy and geochemistry of the late Neogene ocean. *Earth Planet. Sci. Lett.*, 92:165–178.
- Jansen, E., and Sjøholm, J., 1991. Reconstruction of glaciation over the past 6 Myr from ice-borne deposits in the Norwegian Sea. *Nature*, 349:600–603.
- Jansen, E., Sjøholm, J., Bleil, U., and Erichsen, J.A., 1990. Neogene and Pleistocene glaciations in the Northern Hemisphere and late Miocene–Pliocene global ice volume fluctuations: evidence from the Norwegian Sea. In Bleil, U., and Thiede, J. (Eds.), *Geological History of the Polar Oceans: Arctic Versus Antarctic*: Dordrecht (Kluwer), 677–705.
- Kennett, J.P., and Thunell, R.C., 1975. Global increase in Quaternary explosive volcanism. *Science*, 187:497–503.
- Kent, D.V., Opdyke, N.D., and Ewing, M., 1971. Climate change in the North Pacific using ice-raftered detritus as a climatic indicator. *Geol. Soc. Am. Bull.*, 82:2741–2754.
- Krissek, L.A., 1989. Late Cenozoic records of ice-rafting at ODP Sites 642, 643, and 644, Norwegian Sea: onset, chronology, and characteristics of glacial/interglacial fluctuations. In Eldholm, O., Thiede, J., Taylor, E., et al., *Proc. ODP. Sci. Results*, 104: College Station, TX (Ocean Drilling Program), 61–74.
- Krissek, L.A., Morley, J.J., and Lofland, D.K., 1985. The occurrence, abundance, and composition of ice-raftered debris in sediments from Deep Sea Drilling Project Sites 579 and 580, northwest Pacific. In Heath, G.R., Burckle, L.H., et al., *Init. Repts. DSDP*, 86: Washington (U.S. Govt. Printing Office), 647–655.
- Kulm, L.D., von Huene, R., et al., 1973. *Init. Repts. DSDP*, 18: Washington (U.S. Govt. Printing Office).
- Lagoe, M.B., Eyles, C.H., Eyles, N., and Hale, C., 1993. Timing of late Cenozoic tidewater glaciation in the far North Pacific. *Geol. Soc. Am. Bull.*, 105:1542–1560.
- Larsen, H.C., Saunders, A.D., Clift, P.D., Beget, J., Wei, W., Spezzaferri, S., and ODP Leg 152 Scientific Party, 1994. Seven million years of glaciation in Greenland. *Science*, 264:952–955.
- Raymo, M.E., and Ruddiman, W.F., 1992. Tectonic forcing of late Cenozoic climate. *Nature*, 359:117–122.

* Abbreviations for names of organizations and publications in ODP reference lists follow the style given in *Chemical Abstracts Service Source Index* (published by American Chemical Society).

- Raymo, M.E., Ruddiman, W.F., Backman, J., Clement, B.M., and Martinson, D.G., 1989. Late Pliocene variation in Northern Hemisphere ice sheets and North Atlantic deep water circulation. *Paleoceanography*, 4:413–446.
- Raymo, M.E., Ruddiman, W.F., and Clement, B.M., 1987. Pliocene-Pleistocene paleoceanography of the North Atlantic at DSDP Site 609. In Ruddiman, W.F., Kidd, R.B., Thomas, E., et al., *Init. Repts. DSDP*, 94 (Pt. 2): Washington (U.S. Govt. Printing Office), 895–901.
- Raymo, M.E., Ruddiman, W.F., and Froelich, P.N., 1988. Influence of late Cenozoic mountain building on ocean geochemical cycles. *Geology*, 16:649–653.
- Rea, D.K., Basov, I.A., Janecek, T.R., Palmer-Julson, A., et al., 1993. *Proc. ODP Init. Repts.*, 145: College Station, TX (Ocean Drilling Program).
- Rea, D.K., and Schrader, H., 1985. Late Pliocene onset of glaciation: ice-rafting and diatom stratigraphy of North Pacific DSDP cores. *Palaeogeogr., Palaeoclimatol., Palaeoecol.*, 49:313–325.
- Ruddiman, W.F., McIntyre, A., and Raymo, M., 1987. Paleo-environmental results from North Atlantic Sites 607 and 609. In Ruddiman, W.F., Kidd, R.B., Thomas, E., et al., *Init. Repts. DSDP*, 94 (Pt. 2): Washington (U.S. Govt. Printing Office), 855–878.
- Ruddiman, W.F., Raymo, M., and McIntyre, A., 1986. Matuyama 41,000-year cycles: North Atlantic Ocean and Northern Hemisphere ice sheets. *Earth Planet. Sci. Lett.*, 80:117–129.
- Ruddiman, W.F., and Raymo, M.E., 1988. Northern Hemisphere climate regimes during the past 3 Ma: possible tectonic connections. In Shackleton, N.J., West, R.G., and Bowen, D.Q. (Eds.), *The Past Three Million Years*: Evolution of Climatic Variability in the North Atlantic Region: Cambridge (Cambridge Univ. Press), 1–20.
- Shackleton, N.J., Backman, J., Zimmerman, H., Kent, D.V., Hall, M.A., Roberts, D.G., Schnitker, D., Baldauf, J.G., Desprairies, A., Homrighausen, R., Huddlestun, P., Keene, J.B., Kaltenback, A.J., Krumsiek, K.A.O., Morton, A.C., Murray, J.W., and Westberg-Smith, J., 1984. Oxygen isotope calibration of the onset of ice-rafting and history of glaciation in the North Atlantic region. *Nature*, 307:620–623.
- Stewart, R.J., Natland, J.H., and Glassley, W.R., 1973. Petrology of volcanic rocks recovered on DSDP Leg 19 from the North Pacific Ocean and the Bering Sea. In Creager, J.S., Scholl, D.W., et al., *Init. Repts. DSDP*, 19: Washington (U.S. Govt. Printing Office), 615–627.
- von Huene, R., Crouch, J., and Larson, E., 1976. Glacial advance in the Gulf of Alaska area implied by ice-rafted material. In Cline, R.M., and Hays, J.D. (Eds.), *Investigation of Late Quaternary Paleoceanography and Paleoclimatology*. Mem.—Geol. Soc. Am., 145:411–422.
- von Huene, R., Larson, E., and Crouch, J., 1973. Preliminary study of ice-rafted erratics as indicators of glacial advances in the Gulf of Alaska. In Kulm, L.D., von Huene, R., et al., *Init. Repts. DSDP*, 18: Washington (U.S. Govt. Printing Office), 835–842.

Date of initial receipt: 4 April 1994

Date of acceptance: 19 September 1994

Ms 145SR-118

APPENDIX (continued).

Core, section, interval (cm)	Depth (mbsf)	Age (Ma, calculated)	CSD (wt%)	IRD (vol%)	IRD (wt%)	LSR (cm/k.y.)	DBD (g/cm ³)	IRD MAR (g/cm ² /k.y.)
18X-1, 15–17	154.95	5.172	0.43	50.00	0.21	2.63	0.46	0.003
18X-1, 65–67	155.45	5.191	0.16	0.00	0.00	2.63	0.46	0.000
18X-1, 115–117	155.95	5.210	0.10	0.00	0.00	2.63	0.46	0.000
18X-2, 15–17	156.45	5.229	0.35	3.00	0.01	2.63	0.42	0.000
18X-2, 65–67	156.95	5.248	0.12	0.00	0.00	2.63	0.42	0.000
18X-2, 115–117	157.45	5.267	0.11	0.00	0.00	2.63	0.42	0.000
18X-3, 15–17	157.95	5.286	0.21	0.00	0.00	2.63	0.5	0.000
18X-3, 65–67	158.45	5.305	0.15	0.00	0.00	2.63	0.5	0.000
18X-3, 115–117	158.95	5.324	0.09	0.00	0.00	2.63	0.5	0.000
18X-4, 15–17	159.45	5.343	0.14	30.00	0.04	2.63	0.46	0.001
18X-4, 65–67	159.95	5.362	0.11	10.00	0.01	2.63	0.46	0.000
18X-4, 115–117	160.45	5.381	1.12	2.00	0.02	2.63	0.46	0.000
18X-5, 15–17	160.95	5.400	0.04	10.00	0.00	2.63	0.56	0.000
18X-5, 65–67	161.45	5.419	0.18	70.00	0.12	2.63	0.56	0.002
18X-5, 115–117	161.95	5.438	0.16	20.00	0.03	2.63	0.56	0.000
18X-6, 15–17	162.45	5.457	0.20	0.00	0.00	2.63	0.4	0.000
18X-6, 65–67	162.95	5.476	0.31	0.00	0.00	2.63	0.4	0.000

Note: CSD = abundance of the total coarse-sand fraction. IRD = abundance of IRD in the coarse-sand fraction. IRD = abundance of coarse sand-sized IRD in the total sample. LSR = average linear sedimentation rate. DBD = sediment dry-bulk density. IRD MAR = mass accumulation rate of coarse sand-sized IRD.